Int. J. Heat Mass Transfer. Vol. 21, pp. 791–801

0017-9310/78/0601-0791 $02.00/0

THE EFFECT OF BUOYANCY ON FLOW AND HEAT TRANSFER FOR A GAS PASSING DOWN A VERTICAL PIPE AT LOW TURBULENT REYNOLDS NUMBERS

J. P. EASBY
Central Electricity Generating Board, Berkeley Nuclear Laboratories, Berkeley, Gloucestershire, England

(*Received* 22 *June* 1976 *and in revised form* 18 *February* 1977)

Abstract—For the analysis of low-flow situations in the core of the High-Temperature Gas-Cooled reactor it is necessary to have a knowledge of the variation of pressure drop and heat transfer with flow and buoyancy influence. Nitrogen at 4 bar has been used to simulate the high pressure helium in the reactor and an experiment performed for downward flow in a heated vertical pipe.

The measurements show that for the range of flow and buoyancy influence parameters investigated, ($2000 < Re < 10000$ and $Gr < 10^6$), friction factors are reduced by up to 20% compared with a correlation for isothermal flows and heat transfer is increased by up to 40% compared with a correlation for constant fluid properties. Agreement with the limited amount of previous data is quite satisfactory. The changes in heat transfer and friction factor with buoyancy influence can be attributed to distortion of the normally linear, radial shear stress profile. Simple equations have been determined to correlate the present results but extrapolation to conditions of higher flow and buoyancy influence, where the interaction of forced and free convection may be different, is not advised.

NOMENCLATURE

A, channel flow area $= \pi D^2/4$;
a, channel radius;
b, constant;
c, constant;
$C_{1,2,3}$, constants;
Cp, gas specific heat;
D, channel diameter;
f, true friction factor $= 2\tau_w/\rho_B u_B^2$;
f_{iso}, isothermal friction factor;
g, acceleration due to gravity;
Gr, Grashof number $= \dfrac{\rho^2 g D^3 (T_w - T_B)}{\mu^2 T_B}$;
k, gas thermal conductivity;
L, test section or reference length;
m, constant;
$-\Delta P$, test section pressure drop;
Pr, Prandtl number $= \dfrac{Cp\mu}{k}$;
q, heat flux;
r, radial position;
Re, Reynolds number $= WD/\mu A$;
St, Stanton number $= \dfrac{a}{2L}\dfrac{\Delta T}{T_w - T_B}$;
St_{corr}, Stanton number for constant fluid properties;
T, temperature;
T_B, bulk temperature $= \int_0^A \rho u T \, dA \Big/ \int_0^A \rho u \, dA$;
ΔT, test section temperature rise;
u, axial velocity;
u_B, bulk velocity $= \dfrac{1}{A}\int_0^A u \, dA$;
W, gas mass flow rate.

Greek symbols

ρ, gas density;
ρ_B, bulk gas density $= \int_0^A \rho u \, dA \Big/ \int_0^A u \, dA$;
μ, dynamic gas viscosity;
τ, shear stress.

Subscripts

A, evaluated at ambient conditions;
B, evaluated at bulk gas conditions;
w, evaluated at the wall.

Superscript

axial mean.

1. INTRODUCTION

IN THE High-Temperature Gas-Cooled Reactor (HTR) the helium coolant flows vertically downwards through the core. This may present difficulties in the case of operation at very low flow for either fault conditions or low load because the forced downward flow is opposed by a relatively large upward buoyancy force. In order to establish the level of circulator power to maintain flow in the downward direction it is necessary to determine the variations in single-channel pressure drop and heat transfer caused by the radial variation of the buoyancy forces [1].

The differences in fluid properties between helium and nitrogen make it possible to use low-pressure nitrogen to model the buoyancy situation in the reactor. Utilising this fact and using a simple tube geometry, an experimental programme has been carried out to investigate the effects of buoyancy on

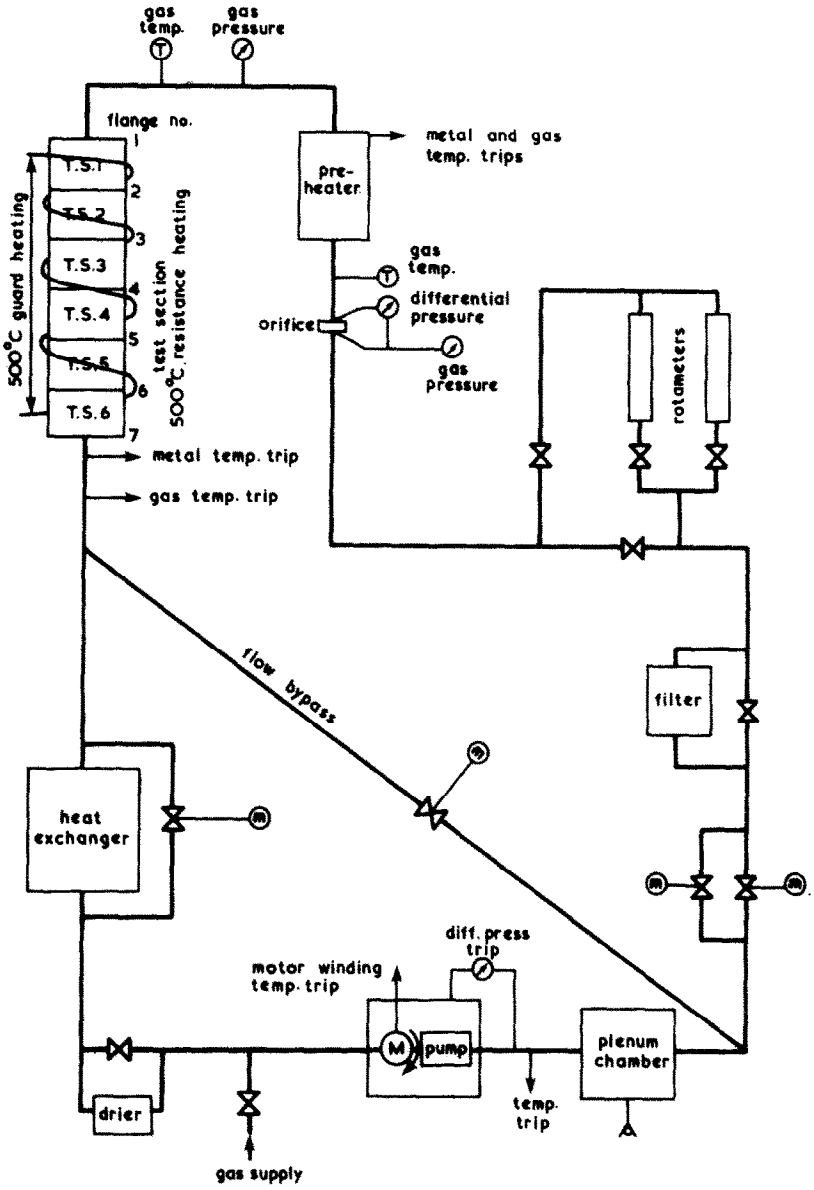

FIG. 1. Schematic diagram of rig.

friction factor, heat transfer and velocity and temperature profiles for a range of turbulent flows.

Measurements have been made for Reynolds numbers between 2000 and 10000 and Grashof numbers up to 10^6.

2. EXPERIMENTAL ARRANGEMENT AND PROCEDURE

The rig consisted of a closed loop around which nitrogen was circulated, see Fig. 1. High-purity nitrogen was supplied via a make-up system to a positive displacement Godfrey type X421 blower. In order to operate at pressures greater than 1 bar, the blower and 10 HP electric motor were enclosed in a steel pressure vessel with the ducting arranged so that the flow into the blower acted as a cooling stream on the motor. The nitrogen at pressures up to 4 bar was circulated through a large plenum chamber, up a vertical pipe containing an orifice plate, down through the test section and eventually back to the circulator. A by-pass loop and three motorised valves enabled test section flow rate to be varied over a wide range. Gas filters and a dryer were provided on by-pass lines. Heat was added to the gas by a preheater as well as by the test section, and removed by a water-cooled heat exchange system. The orifice constants were calculated directly from BS 1042. As a rough check on the calculated calibration, two rotameters, with claimed accuracy 2%, were available to measure mass flow rate.

The test section was fabricated in six equal lengths from 30 mm bore stainless steel tubing, 0.89 mm wall thickness, with flanges induction welded to each end. After welding, the bores were cleaned and measured for distortion. Two 0.79 mm dia holes were drilled diametrically opposite through the flanges to the tube

bore to provide pressure tappings. A probe carrier ring was mounted between each pair of flanges to enable temperature and velocity probes to be inserted into the test section bore. The overall heated length of the test section was 6 m with a 1.5 m unheated entry length.

To measure the test section temperatures, chromel–alumel thermocouples were spot-welded to the outside tube wall of each section. The axial spacing was 25 mm between the first two and then 30 mm for subsequent ones with a ring of four at each end and at the quarter, one half and three quarter length positions making a total of 52 for each test section. All thermocouples were connected to a 500-channel DYNAMCO data logger. The output was via punched paper tape which could then be either printed on a teletype or used as direct input to the IBM 370 computer which processed the results using a purpose-written program.

The pressure tappings at each flange were connected via flexible tubing and a multiple valve switching system to a Combustion Instruments Micromanometer. This instrument was built to a patent design developed by the National Physical Laboratory and based on an idea by Bradshaw [2]. The smallest measurable change in pressure difference was theoretically 0.001 mm w.g. but oscillations in flow and pressure meant that readings to this accuracy were not always possible.

The absolute pressures at the orifice and test section were measured with a Budenberg type pressure gauge and a SE792-50 pressure transducer. Orifice differential pressure was measured with a U-tube type manometer manufactured by Zeal and a Druck PDCR32 pressure transducer. Discrepancies between the pairs of devices were always less than 1% of indicated reading.

The temperature and velocity probes were of a simple pitot tube design. Stainless steel tubing 1.6 mm o.d. and 1.2 mm bore was bent into an L shape to form the pitot-velocity probe. For the temperature probe a thermocouple similar to those used on the test section was inserted in one of the pitot tubes and the thermocouple junction made at the mouth of the tube. For the main programme of testing long-reach probes having a length of order 162 mm in the test section bore were used but for the earlier tests and also for measurement of inlet and outlet gas temperature, relatively short probes, length 30 mm, were used.

The main test section heating was supplied by passing DC from a 20 kVA rectifier through the test section itself. The current supplied was measured via a precision shunt and digital voltmeter and the voltage drop over each test section was measured via a multiple switch and digital voltmeter so enabling the power supplied to be calculated.

The inlet gas temperature could be varied and accurately controlled using a 4.5 kW preheater coupled to an ether controller.

Each test section was lagged to an outside diameter of 245 mm with vermiculite encased in stainless steel covers.

At each flange a pair of guard heater units were used to try and reduce heat loss. These consisted of a labyrinth of pyrotenax heater element embedded in Triton insulating material and encased in a stainless steel half cylinder, the two parts being clipped into place to fit the gap between the main test section lagging.

The main series of tests was performed in two distinct parts. Firstly, with the preheater maintaining a nominal inlet gas temperature of 30°C, ten completely separate tests were performed heating all six test sections. Traversing velocity and temperature probes were inserted at flanges 3, 4 and 6 so that neglecting the first and last section useful measurements were available from four test sections. Secondly, in order to increase the heat rate per unit length but still remain within the temperature limitations of the rig, only the top four test sections were heated and no preheating was applied to the gas. The traversing probe pair from flange 6 was moved up to flange 2 and six tests giving useful measurements over two test sections were performed. Hence, acceptable results from 16 tests were available taken over a pressure range 1–4 bar with a maximum test section temperature of order 530°C and maximum gas outlet temperature of order 420°C. This gave a range of Reynolds numbers from 2000 to 10 000 and Grashof numbers up to 10^6. Table 1 lists the main measured and calculated parameters for each test. A more detailed description of the apparatus and testing procedures is given in Easby [3].

3. ANALYSIS

In order to establish a simple relationship between flow, buoyancy influence and friction factor or Stanton number the results were plotted in the form f/f_{iso} and St/St_{corr} against Gr/Re^2 (the last group arising from the nondimensionalised momentum equation). For Gr/Re^2 tending towards zero, both curves tend towards a value of one and it appears that an equation of first order provides an excellent correlation of the results.

Hence the friction factor equation can be written

$$f/f_{iso} = 1 + C_1 Gr/Re^2$$

and for heat transfer

$$\frac{St}{St_{corr}} = 1 + C_2 \frac{Gr}{Re^2}.$$

For the evaluation of f_{iso}, the correlation due to Drew, Koo and McAdams [4], valid for $3000 < Re \lesssim 10^7$, has been used. This can be written:

$$f_{iso} = 0.125 Re^{-0.32} + 0.0014$$

for heat transfer the correlation:

$$St_{corr} = 0.023 Re^{-0.2} Pr^{-0.6}$$

has been used although there is evidence that for Reynolds numbers less than 10 000 the Stanton numbers should be lower than calculated using this equation (see later in the discussion).

In all the relationships the gas properties have been

Table 1. Main test parameters

Run No.	Test section No.	Mean gas temp. (°C)	Mid test section wall temp. (°C)	Test section pressure (Bar)	Reynolds number Re	Grashof number $Gr \times 10^{-6}$	Friction factor $f \times 10^3$	f/f_{iso}	Stanton number $St \times 10^3$	St/St_{corr}	T_w/T_B	Gr/Re^2
1	2	66.0	106.2	1.84	9426	0.269	8.48	1.049	4.54	1.005	1.119	0.00303
	3	86.5	126.8		9013	0.207	8.39	1.026	4.77	1.045	1.112	0.00254
	4	108.5	145.2		8619	0.144	7.91	0.955	4.66	1.013	1.096	0.00193
	5	129.9	164.0		8278	0.105	8.52	1.018	4.81	1.036	1.084	0.00153
2	2	133.8	231.6	1.82	8208	0.282	8.74	1.042	4.99	1.072	1.240	0.00419
	3	197.2	288.0		7402	0.138	8.62	1.0	4.76	1.057	1.192	0.00252
	4	242.5	339.0		6949	0.0981	8.81	1.004	4.81	0.994	1.187	0.00203
	5	287.1	386.0		6571	0.0701	9.72	1.091	4.93	1.006	1.176	0.00162
3	2	124.8	220.4	3.18	9472	0.927	8.22	1.019	4.93	1.091	1.240	0.0103
	3	184.8	273.1		8564	0.459	7.61	0.917	5.016	1.085	1.193	0.00626
	4	235.3	320.8		7967	0.281	7.80	0.922	4.93	1.049	1.168	0.00442
	5	286.0	366.8		7473	0.176	8.60	1.0	4.90	1.027	1.145	0.0031
4	2	167.95	277.5	3.90	6495	1.013	8.38	0.938	5.88	1.206	1.248	0.0240
	3	242.3	348.7		5831	0.497	8.20	0.891	5.88	1.175	1.206	0.0146
	4	311.1	412.0		5360	0.273	8.69	0.923	5.58	1.092	1.173	0.00951
	5	381.3	465.0		4971	0.139	8.95	0.932	5.60	1.078	1.128	0.00562
5	2	158.7	246.4	3.86	4715	0.873	8.54	0.877	7.11	1.367	1.203	0.0392
	3	232.9	311.0		4222	0.387	8.26	0.822	6.46	1.209	1.154	0.0217
	4	286.4	367.2		3945	0.259	9.16	0.896	6.32	1.165	1.144	0.0166
	5	344.9	412.0		3692	0.139	10.11	0.970	5.94	1.079	1.108	0.0102
6	2	90.96	137.8	3.85	5430	0.996	8.17	0.871	6.50	1.29	1.129	0.0338
	3	126.3	173.0		5069	0.656	8.62	0.903	6.37	1.245	1.117	0.0255
	4	160.2	207.5		4778	0.461	8.79	0.906	5.95	1.148	1.109	0.0202
	5	195.3	235.0		4523	0.274	9.33	0.947	6.02	1.146	1.085	0.0134
7	2	59.1	77.5	3.85	5905	0.592	8.23	0.898	5.85	1.179	1.055	0.0170
	3	74.7	93.8		5701	0.496	8.20	0.887	5.78	1.156	1.055	0.0153
	4	89.1	109.6		5528	0.446	7.96	0.854	5.72	1.137	1.056	0.0146
	5	104.5	122.3		5358	0.321	9.0	0.956	5.65	1.118	1.047	0.0112
8	2	49.7	72.0	1.05	6421	0.0616	9.56	1.068	5.15	1.054	1.069	0.00149
	3	65.2	84.3		6193	0.0426	9.23	1.02	5.04	1.023	1.056	0.00111
	4	74.4	95.6		6067	0.0421	9.02	0.991	4.85	0.982	1.061	0.00114
	5	83.6	105.6		5947	0.0387	9.75	1.066	4.90	0.987	1.061	0.00109
9	2	105.2	170.8	1.05	5611	0.087	9.87	1.063	5.00	0.997	1.173	0.00275
	3	148.6	207.5		5180	0.048	9.59	1.01	5.37	1.052	1.14	0.00178
	4	184.0	242.0		4890	0.033	9.36	0.97	5.38	1.039	1.13	0.00138
	5	220.5	272.5		4636	0.021	10.06	1.027	5.41	1.032	1.11	0.00098
10	2	170.7	287.0	1.026	4918	0.073	10.19	1.058	5.14	0.995	1.262	0.0030
	3	246.6	347.0		4407	0.0314	9.74	0.981	5.61	1.058	1.193	0.0016
	4	311.1	403.0		4075	0.0173	9.60	0.946	5.23	0.969	1.157	0.0010
	5	374.0	451.0		3806	0.0093	10.33	1.0	5.63	1.028	1.119	0.0006
11	2	232.6	360.0	4.0	4219	0.682	8.04	0.80	7.08	1.326	1.252	0.0383
	3	348.8	459.7		3673	0.242	8.85	0.848	6.45	1.169	1.178	0.0179
12	2	258.6	389.0	1.93	2362	0.130	11.12	0.94	7.0	1.165	1.245	0.0234
	3	365.2	474.0		2090	0.049	11.08	0.91	6.68	1.08	1.171	0.0113
13	2	228.2	389.0	2.0	5057	0.223	9.15	0.957	5.68	1.103	1.321	0.0087
	3	343.4	476.5		4400	0.075	9.35	0.942	5.55	1.043	1.216	0.0038
14	2	210.4	373.0	3.0	7540	0.598	7.86	0.916	5.33	1.123	1.336	0.0105
	3	321.3	463.0		6559	0.212	8.16	0.916	5.21	1.062	1.238	0.0049
15	2	268.0	390.0	4.0	3395	0.486	8.66	0.812	7.78	1.392	1.226	0.0422
	3	389.7	496.0		2966	0.176	9.19	0.829	6.84	1.187	1.160	0.0199
16	2	200.5	322.5	4.0	5185	0.866	7.91	0.833	6.82	1.334	1.257	0.0322
	3	303.0	413.0		4541	0.333	9.11	0.926	6.18	1.171	1.191	0.0161

evaluated at the bulk fluid temperature at mid test section using nitrogen properties recommended by the National Engineering Laboratory, Watson [5].

The momentum–impulse balance for the steady downward flow of an ideal gas at low Mach number gives the following equation, from which friction factors were calculated for each test section:

$$f = \frac{\bar{\rho} A^2 a}{W^2}\left(\bar{\rho} g + \frac{\Delta P}{L}\right) - \frac{a}{T_B}\frac{\Delta T}{L}. \quad (1)$$

A correction was applied to the measured pressure drop to allow for the difference in densities of the fluid in the test section and the manometer lines.

Because of the uncertainties involved in evaluating heat losses the Stanton number for each test section was evaluated as:

$$St = \frac{a\Delta T}{2(T_w - T_B)L}$$

where ΔT is the rise in gas temperature over the length L and $T_w - T_B$ is the wall-to-gas bulk temperature difference. From plots of wall temperature variation

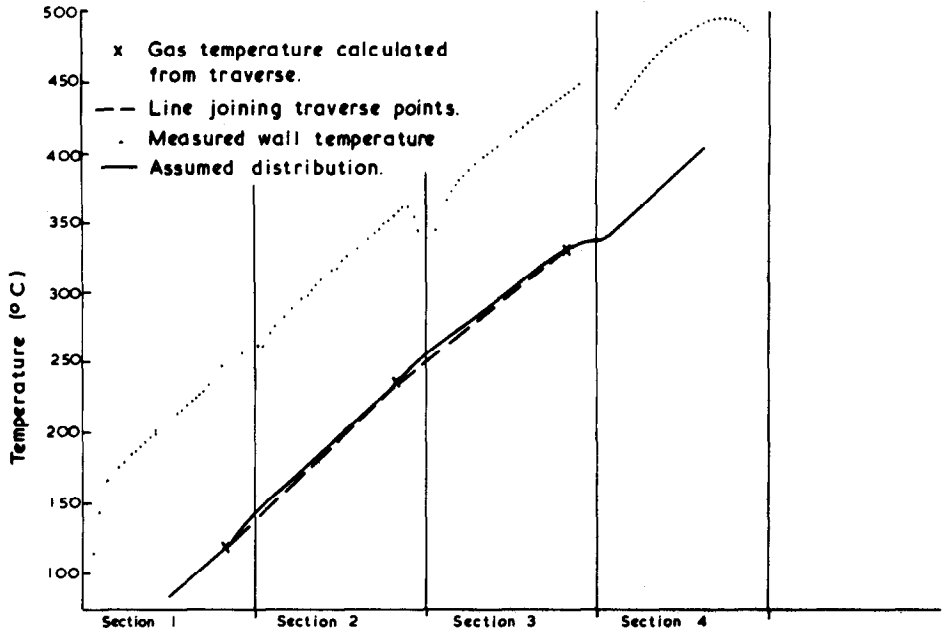

FIG. 2. Measured and assumed temperature distributions for calculation of parameters (four test sections heated).

with axial position and the bulk gas temperatures evaluated at the traverse positions it was possible to calculate the denominator of the equation. The numerator was evaluated by assuming that the gas temperature rise over the length of channel from the midpoint to the traverse plane would be identical to the tube wall temperature gradient estimated over the same length. This method of calculating $\Delta T/L$ was deemed more accurate than taking the gradient between successive temperature traverses because of the non-linear variation of gas temperature in the region of the flanges. However, in general there was very little difference between the two gradients, see Fig. 2. When there were six test sections heated, for test section four there were no traversing probes and it was necessary to estimate the required bulk gas temperature from the axial gas temperature gradient from test sections 3–5.

The values of bulk temperature and mass flow rate from the traverses were obtained by numerical integration of the profiles using linear interpolation between points. Agreement with the mass flow rate measured by the orifice plate was usually within the range -6% and $+3\%$.

The individual velocities were calculated from the pressure difference measured by the micromanometer between the pitot probe and a flange pressure tapping with allowance made for channel pressure drop and density differences in manometer lines. A correction was made as suggested by MacMillan [6] for the effect of the wall on the measured velocity but since the pitot Reynolds number was always greater than ~ 50 it was not considered necessary to make a further correction for viscous effects, MacMillan [7].

Following an experimental investigation with a radiation-shielded temperature probe in which very little discrepancy was found from the measurements with the type of probe used in the main programme of tests it was decided that no correction would be applied to the individual temperature readings.

4. RESULTS AND DISCUSSION

4.1. *Profiles*

The effect of the buoyancy forces on the profiles of velocity and temperature across the pipe is shown in Figs. 3 and 4. The velocity nondimensionalised by the bulk velocity, u_B, is plotted against radial position in Fig. 3 for each of the three traverses of two runs with similar Reynolds numbers but Grashof numbers an order of magnitude different. The figure is representative of the general trend that as the Grashof number increases, for a constant Reynolds number, the centre line velocity increases, the profile thus tending to become more peaked.

Figure 4 shows the corresponding distribution of dimensionless temperature expressed as $T_w - T/T_w - T_B$. The profiles become flatter with increasing buoyancy influence and in general the gradient near the wall is increased, but because of the physical size of the traversing probes it is impossible to draw any firm conclusions in this region. However, no gross distortion in the profiles of either velocity or temperature were measured in the present experiments up to the maximum value of $Gr/Re^2 \sim 0.05$.

Similar velocity profiles to those in the present experiment, tending to a more peaked shape as the buoyancy influence increased but showing no large distortions, were measured by Axcell [8] for air flowing down a large diameter duct. For turbulent upflow in the same rig, Byrne and Ejiogu [9] measured large distortions of velocity profiles near the wall with

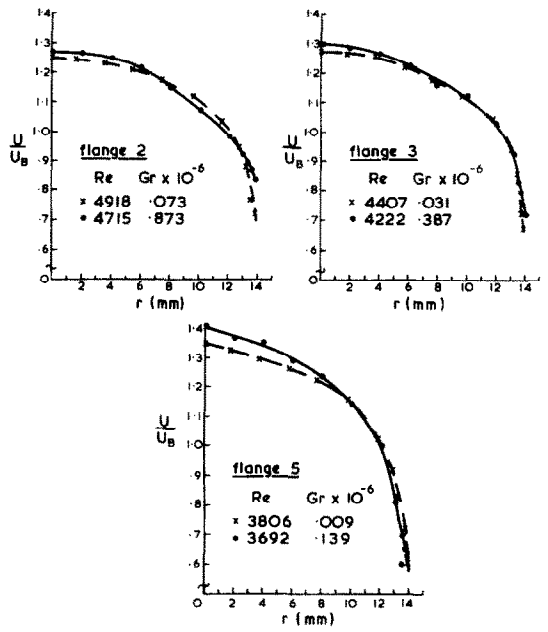

FIG. 3. Velocity profiles for two runs with similar Reynolds numbers but different Grashof numbers.

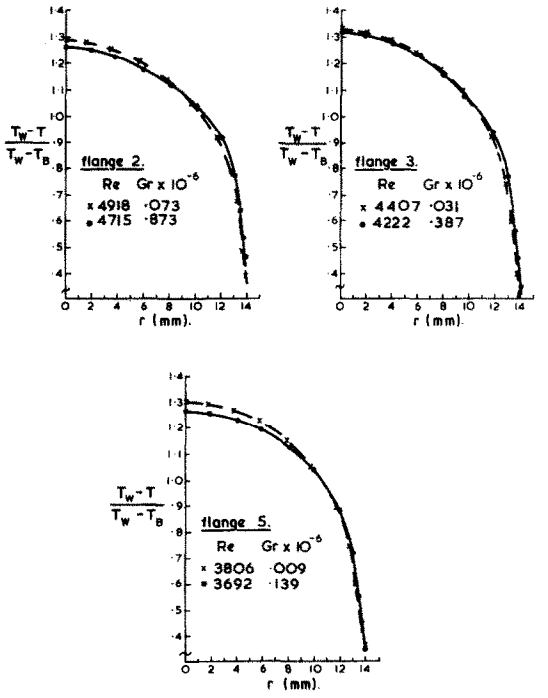

FIG. 4. Temperature profiles for two runs with similar Reynolds numbers but different Grashof numbers.

$Gr/Re^2 \gtrsim 0.2$. However, since the duct was of such a large diameter, the length to diameter ratio was very low and it has been observed by other investigators, Brown and Gauvin [10] that in upflow the flow is subject to large distortion over quite a large region, whereas in downflow the flow field becomes extremely stable in a few diameters. Hence, there seems to be a consistent pattern in the measurements from all these investigations.

Carr, Connor and Buhr [11] show that for turbulent upflow at $Gr/Re^2 \lesssim 0.04$ there is very little change in the profiles of both temperature and velocity when compared with results for low heat rates. However at $Gr/Re^2 \gtrsim 0.06$ their velocity profiles are becoming much steeper near the wall and flat in the centre of the duct with a maximum value in velocity occurring away from the centre line. This flattening of the velocity profile in upflow obviously corresponds to the peaking observed for the same Gr/Re^2 for the present downflow experiments.

Several other investigations present temperature or velocity profiles but no comparison is made here because in general they are for laminar flow with much higher values of Gr/Re^2 than the present experiment. However, from the comparisons made with the references quoted above there is reasonable agreement in trends.

4.2. *Friction factors*

The variation of isothermal friction factor for the test sections with all probes in position is shown in Fig. 5 together with the correlation of Drew, Koo and McAdams. The general scatter about this line is of order $+8\%$ to -5% with one or two sets of points exhibiting much larger scatter. This can be attributed to two causes. Firstly, the differential pressures being measured were extremely low and in some cases they approached the limits of the micromanometer. Secondly, no corrections have been applied to the unheated runs for changes in density in the manometer pressure lines caused by changes in ambient temperature. This was a shortcoming of the early experimental procedure which was rectified for the heated measurements.

The true friction factors from the heated tests evaluated as outlined in Section 3 are plotted in Fig. 6 as f/f_{iso} against Gr/Re^2.

The general trend is that friction factors are reduced by the effects of the buoyancy forces. A least mean squares line fitted to the data gives the relationship:

$$\frac{f}{f_{iso}} = 1.006 - 5.13 Gr/Re^2$$

with a percentage residual standard deviation of $\sim 5\%$.

The results for test Section 2 with six test sections heated appear to be consistently high. Similarly, Section 3 with four test sections heated is consistently low. This would seem to indicate that these test sections had higher and lower isothermal friction factors than the Drew, Koo and McAdams correlation, especially since the gradient of lines drawn through these two sets of points is virtually identical to the overall mean line gradient in Fig. 6. However, no definite trend is obvious from the isothermal results, so all heated results have been normalised with respect to the one correlation.

The measured reduction in friction factor can be attributed to the change in velocity profile that must occur as the buoyancy forces increase. Figure 7 shows the probable velocity profiles for a given bulk velocity

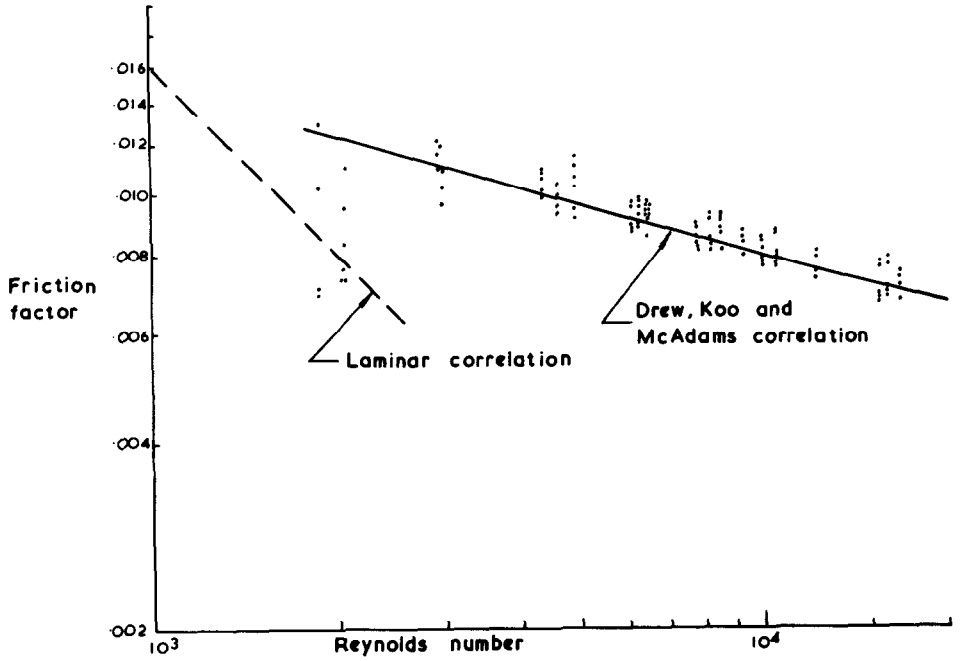

FIG. 5. Isothermal friction factors.

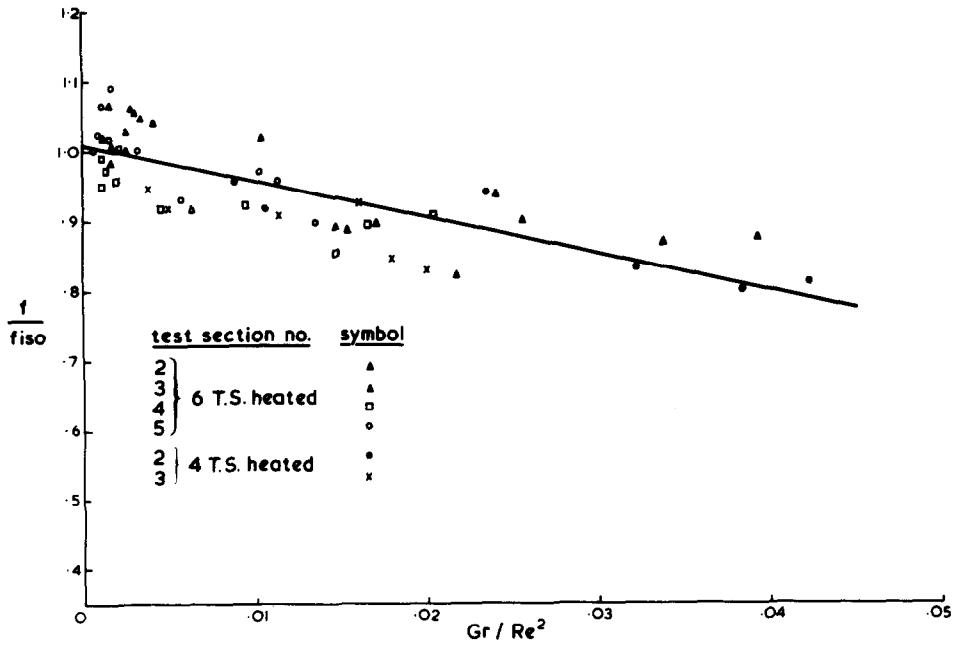

FIG. 6. Variation of friction factor with buoyancy influence.

and changing Grashof numbers. Such distributions have been calculated for laminar flow by Hanratty, Rosen and Kabel [12] and Brown [13]. There eventually becomes a point when the velocity gradient at the wall is zero and from the definition:

$$f \equiv 2\tau_w/\rho_B u_B^2 = -2\mu_w \frac{\mathrm{d}u}{\mathrm{d}r}\bigg|_w \Big/ \rho_B u_B^2,$$

this implies a zero friction factor. Obviously the use of isothermal friction factor data for design purposes becomes increasingly unreliable as the free convection component increases in relation to the forced one. However, for the present range with no great distortion in the profiles, the comparison with isothermal friction factors provided by the correlation is extremely interesting.

4.3. *Heat transfer*

Numerous investigations into the effect of high heat rates on heat transfer have suggested correlations of the form:

$$St = C_3 Re^b Pr^c \left(\frac{T_w}{T_B}\right)^m.$$

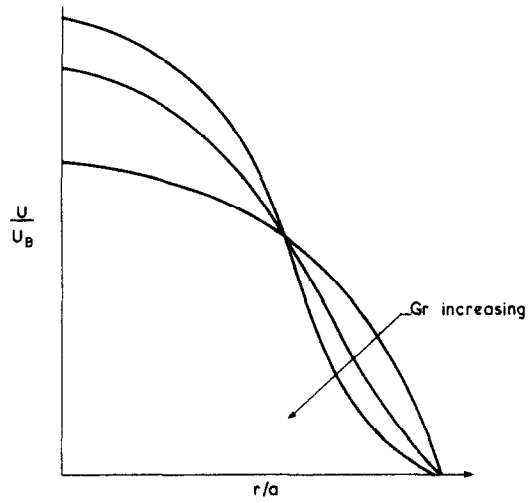

FIG. 7. Probable velocity distribution with increasing buoyancy influence.

Other suggested correlations have involved density or viscosity ratios or even reference temperatures different from the bulk temperature usually used to evaluate the gas properties. However, correlations of this type are an attempt to account for variations in all the physical properties rather than the effects of buoyancy.

Eckert and Diaguila [14] establish criteria for upflow to decide whether a flow is dominated by free or forced convection or is in the mixed convection regime but do not offer a correlation for this last alternative. Having established that the present results are in a mixed convection or buoyancy influenced region, the Dittus Boelter correlation for heat transfer with constant fluid properties has been used as a comparison with the measured buoyancy influenced Stanton number. Hence Fig. 8 is a plot of St/St_{corr} against Gr/Re^2 with $St_{corr} = 0.023Re^{-0.2}Pr^{-0.6}$.

It would have been more correct to apply a factor $(T_w/T_B)^m$ to both St_{corr} and f_{iso}. However, it was found that for heat transfer, this factor increased the scatter about the mean line. For friction factor the effect is uncertain but relatively small, so that neither correction has in fact been used.

The least-mean-squares line fitted to the results with a percentage residual standard deviation of $\sim 2\%$ is

$$St/St_{corr} = 1.009 + 8.91 Gr/Re^2.$$

There is considerable uncertainty in Stanton number correlations at low heat rates for Reynolds numbers below 10^4. The Engineering Sciences Data Unit (Item No. 67016) recommends a correlation which falls below the Dittus Boelter correlation by greater than 10%. However, the present results at low heat rates tend towards a St/St_{corr} value of 1 and seem to confirm the use of this correlation for comparison purposes.

A number of previous investigations have measured large increases in heat transfer for buoyancy influenced downflow. Brown and Gauvin [15, 10] measured an increase of order 70% in heat transfer, compared with the constant properties correlation quoted above, for heat transfer to air at Grashof numbers rather larger but Reynolds numbers similar to those of the present experiment, giving a $Gr/Re^2 \simeq 0.2$. In evaluating the nondimensional parameters they used gas properties calculated at a film temperature in the Grashof and Reynolds number but at the wall temperature in the Nusselt number. Hence it is probable that the increase in heat transfer when evaluated in the same way as the present results is much larger than this figure. If the present correlation was extended to $Gr/Re^2 = 0.2$ the predicted improvement would be greater than 100%. Brown and Gauvin suggest that the improvement they

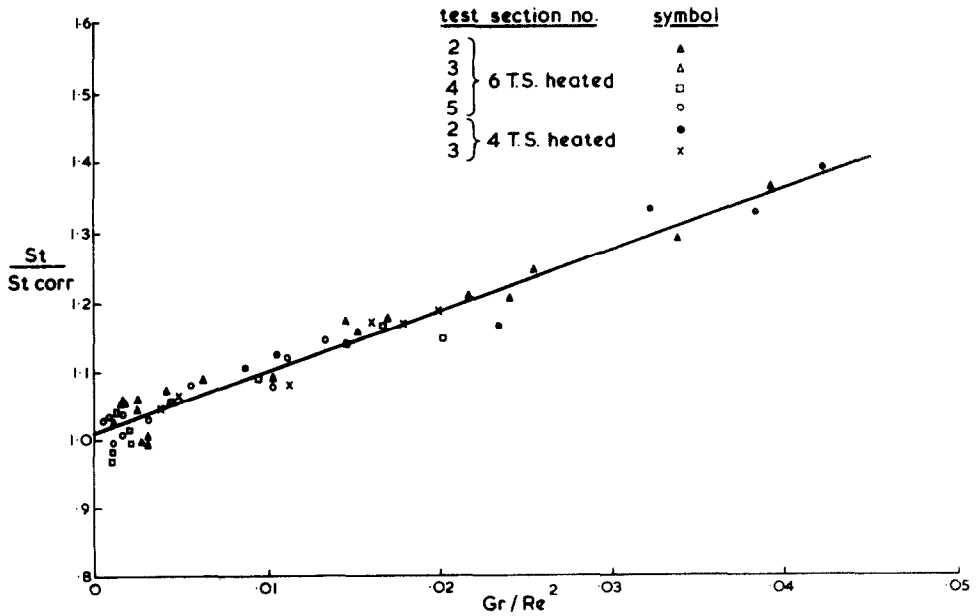

FIG. 8. Variation of Stanton number with buoyancy influence.

measured can be attributed to the change in turbulent transport resulting from the relatively large temperature fluctuations they measured and an increase in the correlation coefficient between the radial velocity and temperature fluctuations.

The results of Herbert and Sterns [16] for downflow of water indicate a maximum increase of 40% in Nusselt number for similar Reynolds numbers but much larger Grashof numbers than the present results. However, they also have used a different reference temperature for evaluating the properties in the dimensionless parameters. Using approximate conversions from film to bulk properties it would seem that the greatest increase could be 100% and for a value of Gr/Re^2 comparable to the highest attained in the present tests the increase was of order 50%.

Axcell [8] gives the results of his own experiments for downflow of air in a large-diameter pipe and also mentions other downflow work performed at Manchester University on supercritical CO_2 in a small-diameter pipe and water at atmospheric pressure in a large-diameter pipe. Extremely large increases in heat transfer were measured for both Grashof and Reynolds number larger than in the present experiment. From considerations of the buoyancy effect on the shear stress profile in upflow (Hall and Jackson [17]), he quotes a formula which provides a reasonable correlation of data from all three experiments but the air data for the lowest Reynolds numbers (2×10^4) are higher than the predicted values. Later work from Manchester, Jackson and Fewster [18], gives an improved correlation fitted to their own and other investigators' data on heat transfer to water. The increases in heat transfer do not seem to be as large as those measured in the present experiment for the same grouping of dimensionless numbers, even taking into account the different definitions of Grashof number. However, extremely large increases were measured and any differences between the sets of data may be due to the different ranges of Grashof and Reynolds number as well as differences in the fluid used.

The most likely explanation of the increases in heat transfer which occur in all these experiments can be deduced by examining the variation of shear stress across the pipe. For an unheated flow the relationship between shear stress and radial position is linear. However, as the influence of buoyancy increases, in downflow the wall shear stress decreases but the profile becomes greatly distorted and there is a shear stress maximum away from the wall, in the region where energy is fed into the turbulence. Figure 9 shows the shear stress profile for a run at high Grashof number and low Reynolds number. It was calculated using the velocity and temperature traverse data from the present experimental results by using the following equation which can be deduced from a simplified x-momentum and overall momentum balance:

$$\tau = \frac{1}{r}\int_0^r \left(\rho_B u_B \frac{\mathrm{d}u_B}{\mathrm{d}x} - \rho u \frac{\partial u}{\partial x} - (\rho_B - \rho)g + 2\tau_w/a\right) r\,\mathrm{d}r.$$

In the region of maximum shear stress the production of turbulence energy, expressed as $\tau\,\mathrm{d}u/\mathrm{d}y$ will be much larger than with a normal shear stress profile and hence the eddy diffusivities of heat and momentum will be increased. This in turn will result in much higher transfer of heat in the region and be reflected in the large increases in Stanton number. Axcell's calculations of the eddy diffusivity of heat from his results and the turbulence measurements presented by Brown and Gauvin confirm this mechanism. Further indirect support is provided by the upflow measurements of Carr, Connors and Buhr [11]. They show the shear stress becoming much less in the region of maximum turbulence production as buoyancy increases and Nusselt numbers deduced from their measurements are correspondingly much lower than the low heat-rate correlation values. A number of other investigations of upflow have shown decreases in heat transfer with increasing buoyancy influence. Hall and Jackson [17] suggest a mechanism as above based on the shear stress variation to explain their results for supercritical CO_2.

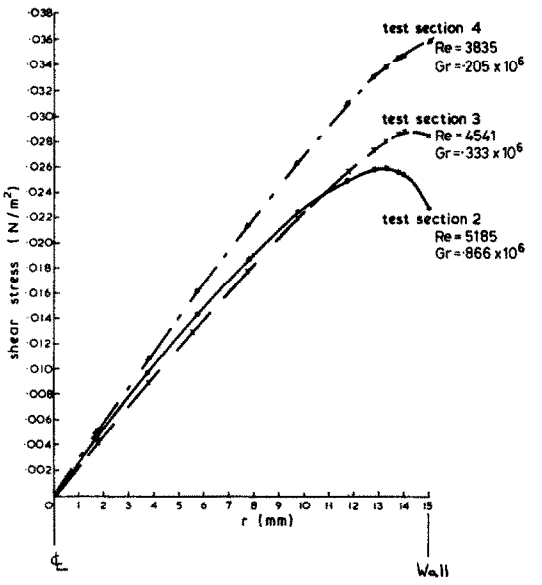

FIG. 9. Shear stress distribution calculated for a high Grashof number, low Reynolds number run.

5. CONCLUSIONS

The present experiments for turbulent downflow of nitrogen in a tube with buoyancy influence for $2000 < Re < 10\,000$ and $Gr \lesssim 10^6$ have shown that:

(1) Friction factors are reduced by up to 20% compared with the correlation of Drew, Koo and McAdams for isothermal flow.

(2) The effects of buoyancy on friction factors can be correlated for the present range of conditions by the relationship

$$f/f_{\mathrm{iso}} \simeq 1 - 5.1\,Gr/Re^2.$$

(3) Stanton numbers are increased by up to 40% compared with the correlation for constant properties. Agreement with previous investigations is satisfactory.

(4) Stanton numbers are correlated by the relationship

$$St/St_{corr} = 1 + 8.9Gr/Re^2.$$

(5) The increase in Stanton number and decrease in friction factor can be explained by the effect of the buoyancy forces on the shear stress distribution across the pipe. With increasing buoyancy the velocity gradient at the wall is reduced resulting in a decreased wall shear stress and friction factor. The shear stress in the region of maximum turbulence production is greatly increased resulting in higher eddy diffusivities and hence an increased Stanton number.

Acknowledgement—This paper is published by permission of the Central Electricity Generating Board.

REFERENCES

1. C. J. Lawn and D. Withrington, Conditions leading to flow reversal in a downflow core, ASME Paper No. 74-WA/HT-63 (1974).
2. P. Bradshaw, A compact, null reading, tilting U-tube micromanometer with a rigid liquid container, *J. Scient. Instrum.* **42**, 677–680 (1965).
3. J. P. Easby, The effect of buoyancy on flow and heat transfer for a gas passing down a vertical pipe at low turbulent Reynolds numbers, CEGB Report No. RD/-B/N3507 (1976).
4. T. B. Drew, E. C. Koo and W. H. McAdams, The friction factor for clean round tubes, *Trans. Am. Inst. Chem. Engrs* **28**, 56–72 (1932).
5. J. T. R. Watson, Viscosity of gases in metric units. NEL, HMSO (1972).
6. F. A. MacMillan, Experiments on pitot-tubes in shear flow, A.R.C. Report No. 3028 (1956).
7. F. A. MacMillan, Viscous effects on pitot tubes at low speeds, *J. R. Aero. Soc.* **58**, 570–572 (1954).
8. B. P. Axcell, The effect of buoyancy on forced convection heat transfer. Ph.D. Thesis, University of Manchester (1975).
9. J. F. Byrne and E. Ejiogu, Combined free and forced convection heat transfer in a vertical pipe, Paper C118/71, *Symposium on Heat and Mass Transfer by Combined Forced and Natural Convection*, Inst. Mech. Engrs (1971).
10. C. K. Brown and W. H. Gauvin, Temperature profiles and fluctuations in combined free and forced convection flows, *Chem. Engng Sci.* **21**, 961–970 (1966).
11. A. D. Carr, M. A. Connor and H. O. Buhr, Velocity, temperature and turbulence measurements in air for pipe flow with combined free and forced convection, *J. Heat Transfer* **95**, 445–452 (1973).
12. T. J. Hanratty, E. M. Rosen and R. L. Kabel, Effect of heat transfer on flow field at low Reynolds numbers in vertical tubes, *Ind. Engng Chem.* **50**, 815–820 (1958).
13. W. G. Brown, Die Überlagerung von Erzwungener und Natürlicher Konvektion bei Niedrigen Durchsätzen in Einem Lotrechten Rohr, *ForschungsHft. Ver. Dt. Ing.*, 480 (1960).
14. E. R. G. Eckert and A. J. Diaguila, Convective heat transfer for mixed, free and forced flow through tubes, ASME Paper No. 53-A191 (1954).
15. C. K. Brown and W. H. Gauvin, Combined free and forced convection, *Can. J. Chem. Engng* **43**, 306–318 (1965).
16. L. S. Herbert and U. J. Sterns, Heat transfer in vertical tubes—interaction of forced and free convection, *Chem. Engng Jl* **4**, 46–52 (1972).
17. W. B. Hall and J. D. Jackson, Laminarization of a turbulent pipe flow by buoyancy forces, ASME Paper No. 69-HT-55 (1969).
18. J. D. Jackson and J. Fewster, Enhancement of turbulent heat transfer due to buoyancy for downward flow of water in vertical tubes, International Seminar Beograd (1976).

L'EFFET DES FORCES D'ARCHIMEDE SUR L'ECOULEMENT ET LE TRANSFERT THERMIQUE POUR UN GAZ DESCENDANT DANS UN TUBE VERTICAL A DEUX NOMBRES DE REYNOLDS TURBULENTS

Résumé—Dans l'analyse des situations d'écoulement dans le coeur d'un réacteur à haute température refroidi par un gaz, il est nécessaire de connaitre la variation de la chute de pression et le transfert thermique en fonction du débit et de la gravité. On utilise l'azote sous 4 bar pour simuler l'hélium à haute pression dans le réacteur et une expérimentation est conduite avec un écoulement descendant dans un tube chaud vertical. Les mesures montrent que, dans le domaine des débits et des forces d'Archimède considéré ($2000 < Re < 10\,000$ et $Gr < 10^6$), des coefficients de frottement sont réduits de 20%, en comparaison des valeurs pour les écoulements isothermes et le transfert thermique est accru de 40% par rapport au cas des propriétés constantes de fluide. L'accord avec les données connues, en nombre limité, est tout à fait satisfaisant. Les changements dans le transfert thermique et dans le frottement sous l'influence de l'effet de la gravité peuvent être attribués à une distorsion du profil radial de tension de cisaillement généralement linéaire. Des équations simples ont été déterminées pour rassembler les présents résultats mais il n'est pas recommandé d'extrapoler à des conditions de grands débits et de forte influence de pesanteur car l'interaction des convections forcée et naturelle peut être différente.

DER EINFLUSS DES AUFTRIEBS AUF DIE STRÖMUNG UND DEN WÄRMEÜBERGANG BEI DER TURBULENTEN, ABWÄRTS GERICHTETEN STRÖMUNG EINES GASES BEI KLEINEN *RE*-ZAHLEN

Zusammenfassung—Für die Berechnung von Vorgängen mit langsamer Strömung im Kern des gasgekühlten Hochtemperaturreaktors ist es notwendig, die Änderung des Druckverlustes und des Wärmeübergangs mit dem Strömungs- und Auftriebseinfluß zu kennen. Für die Simulation des Hochdruckheliums im Reaktor wurde Stickstoff von 4 bar verwendet. Es wurden Versuche bei abwärts gerichteter Strömung in einem beheizten senkrechten Rohr durchgeführt. Die Messungen zeigen, daß im untersuchten Strömungs- und Auftriebsbereich ($2000 < Re < 10\,000$ und $Gr < 10^6$) die Reibungsfaktoren um bis zu 20% geringer waren.

verglichen mit einer Beziehung für isotherme Strömungen. Außerdem erhöhte sich der Wärmeübergang um bis zu 40%, verglichen mit einer Beziehung für konstante Fluideigenschaften. Die Übereinstimmung mit der begrenzten Anzahl bisheriger Daten ist recht zufriedenstellend. Die Änderungen des Wärmeübergangs und des Reibungsfaktors mit dem Auftriebseinfluß kann auf die Verformung des gewöhnlich linearen radialen Schubspannungsprofils zurückgeführt werden. Es wurden einfache Gleichungen entwickelt, um die gegenwärtigen Ergebnisse zu korrelieren. Die Extrapolation auf Bedingungen mit größerem Strömungs- und Auftriebseinfluß, bei denen das Zusammenwirken der erzwungenen und der freien Konvektion anders sein kann, ist nicht ratsam.

ВЛИЯНИЕ АРХИМЕДОВЫХ СИЛ НА ТЕЧЕНИЕ И ПЕРЕНОС ТЕПЛА В ГАЗЕ, ДВИЖУЩЕМСЯ ПО ВЕРТИКАЛЬНОЙ ТРУБЕ В НАПРАВЛЕНИИ УСКОРЕНИЯ СИЛЫ ТЯЖЕСТИ ПРИ НИЗКИХ ТУРБУЛЕНТНЫХ ЧИСЛАХ РЕЙНОЛЬДСА

Аннотация — Для анализа низкоскоростных процессов в активной зоне высокотемпературного газоохлаждаемого реактора необходимо знать изменения трения и теплообмена в зависимости от течения и влияния архимедовых сил. Для моделирования гелиевого реактора большого давления был использован азот с давлением в 4 бара; эксперимент проводился в нагреваемой вертикальной трубе. Измерения показывают, что в исследованном диапазоне параметров потока и плавучести ($2000 < R < 1000$ и $Gr < 10^6$), коэффициенты трения уменьшаются до 20% по сравнению с соответствующими коэффициентами для изотермических потоков, а теплообмен увеличивается до 40% по сравнению со случаем течения жидкости с постоянными физическими свойствами. Результаты работы вполне удовлетворительно согласуются с имеющимися данными. Изменения в коэффициентах теплообмена и трения под влиянием архимедовых сил могут быть объяснены деформацией обычно линейного радиального профиля касательных напряжений. Были выведены простые уравнения для согласования представленных результатов, однако их экстраполяция на случаи более скоростных потоков и более сильного влияния архимедовых сил, где взаимодействие вынужденной и свободной конвекции может быть иным, проанализирована не была.